Molecular Biology of the Cell
Vol. 18, 4637–4647, November 2007

Analysis of De Novo Golgi Complex Formation after Enzyme-based Inactivation

Florence Jollivet,*† Graça Raposo,*† Ariane Dimitrov,*† Rachid Sougrat,‡ Bruno Goud,*† and Franck Perez*†

*Centre National de la Recherche Scientifique Unité Mixte de Recherche 144, 75248 Paris Cedex 05, France; †Institut Curie, 75248 Paris Cedex 05, France; and ‡Cell Biology and Metabolism Branch, National Institute of Child Health and Human Development, National Institutes of Health, Bethesda, MD 20892-5430

Submitted August 19, 2007; Accepted August 31, 2007
Monitoring Editor: Sandra Schmid

The Golgi complex is characterized by its unique morphology of closely apposed flattened cisternae that persists despite the large quantity of lipids and proteins that transit bidirectionally. Whether such a structure is maintained through endoplasmic reticulum (ER)-based recycling and auto-organization or whether it depends on a permanent Golgi structure is strongly debated. To further study Golgi maintenance in interphase cells, we developed a method allowing for a drug-free inactivation of Golgi dynamics and function in living cells. After Golgi inactivation, a new Golgi-like structure, containing only certain Golgi markers and newly synthesized cargos, was produced. However, this structure did not acquire a normal Golgi architecture and was unable to ensure a normal trafficking activity. This suggests an integrative model for Golgi maintenance in interphase where the ER is able to autonomously produce Golgi-like structures that need pre-existing Golgi complexes to be organized as morphologically normal and active Golgi elements.

INTRODUCTION

One important characteristic of eukaryotic cells is the presence of organelles, and in particular of membrane bound compartments, allowing, for example, spatial restriction of specific enzymatic reactions (e.g., in the mitochondria, lysosomes, peroxisomes) and to finely regulate interactions with the extracellular environment (e.g., changes in stress, growth, polarity). To understand the regulation of eukaryotic cell physiology, cell dynamics have thus to be considered in the context of organelle dynamics. This is particularly evident during cell division, when cell organization is strongly affected. Organelle function has then to be inherited by both daughter cells upon mitosis exit (Warren and Wickner, 1996). During interphase, organelle damage, intracellular remodeling, or simply cellular activity also necessitates a precise control of organelle dynamics. How the organelles are built, maintained, and degraded thus represent key questions that remain unsolved for most organelles.

One particularly studied example is the dynamics of the Golgi apparatus. The Golgi complex play a central role in eukaryotic cell homeostasis. It processes and sorts proteins and lipids synthesized in the endoplasmic reticulum (ER) and serves as a central platform connecting the anterograde and retrograde trafficking pathways. These activities are coupled to unique ultrastructural characteristics. The Golgi apparatus is composed of stacks of flattened, adherent cisternae (Rambourg and Clermont, 1997; Ladinsky *et al.*, 1999). In certain eukaryotes, and in particular in humans, hundreds of stacks are laterally connected to form an extended ribbon-like structure next to the microtubule-organizing center (MTOC). Each stack displays an internal polarity: the *cis* side exchanges material from the ER through the intermediate compartment and the *cis*-Golgi network; at the other extremity, the *trans*-Golgi, separated from the *cis*-Golgi by intervening medial cisternae, is in contact with the *trans*-Golgi network (TGN). The TGN executes final sorting steps to target multiple post-Golgi destinations and exchanges material with the endocytic pathway.

Despite the large and continuous flow of membranes and proteins occurring at steady state, the overall organization, ultrastructural shape, and polarity of the Golgi apparatus is remarkably stable. Each Golgi cisternae contains a particular set of "resident" proteins, such as glycosylation enzymes, but how this is maintained is still debated (Martinez-Menarguez *et al.*, 2001; Cosson *et al.*, 2002; Altan-Bonnet *et al.*, 2004; Puthenveedu and Linstedt, 2005; Storrie, 2005). Two extreme models have been proposed to explain how such a structure is dynamically maintained. According to the "static cisternae" model, cargo advances, packed in vesicles or using extended tubules, through a stable stacked structure (Pelham, 2001). According to this model, resident proteins are stably localized to particular cisternae using specific signals, through interactions with the membranes or with the matrix, a sort of stable and inheritable exoskeleton that may serve as a template for the maintenance of the Golgi complex. This matrix is particularly important upon mitosis exit (Shorter and Warren, 2002) but is also proposed to play a role during interphase to maintain Golgi structure (reviewed in Glick, 2002). According to the "cisternal mat-

This article was published online ahead of print in *MBC in Press* (http://www.molbiolcell.org/cgi/doi/10.1091/mbc.E07–08–0799) on September 12, 2007.

Address correspondence to: Franck Perez (Franck.Perez@curie.fr).

Abbreviations used: BFA, brefeldin A; DAB, 3,3′-diaminobenzidine; EM, electron microscopy; EGFP, enhanced green fluorescent protein; EndoH, endoglycosidase H; ER, endoplasmic reticulum; FACS, fluorescence-activated cell sorting; HRP, horseradish peroxidase; ManII, mannosidase II; TGN, *trans*-Golgi network; VSV-G, vesicular stomatitis virus G protein.

uration" model, the Golgi apparatus in endowed with auto-organization abilities and does not depend on an external matrix to build and maintain its structure. Cargo are transported inside maturating cisternae and resident proteins achieve their steady-state localization through retrograde transportation (reviewed in Glick, 2002; Shorter and Warren, 2002; Barr, 2004). Independently of the model, intercisternae transport (respectively of cargo or of resident proteins) may occur via vesicular or tubular connections (for reviews see Mironov *et al.*, 2005; Rabouille and Klumperman, 2005).

Recent studies strongly support the model of cisternal maturation for yeast *Saccharomyces cerevisiae* (Losev *et al.*, 2006; Matsuura-Tokita *et al.*, 2006). In higher eukaryotes, many studies have tried to address the question of Golgi apparatus dynamics using in vivo imaging of green fluorescent protein (GFP)-tagged reporters, recovery from drug treatments, or Golgi re-formation after mitosis (Shima *et al.*, 1997; Zaal *et al.*, 1999; Jokitalo *et al.*, 2001; Puri and Linstedt, 2003; Axelsson and Warren, 2004; Nizak *et al.*, 2004; Pecot and Malhotra, 2004). Few studies, however, have directly addressed the question of Golgi apparatus maintenance in mammalian interphase cells (see however, Pecot and Malhotra, 2006). One way to study it would be to remove the Golgi from living cells and study recovery. Such an idea was followed using cytoplast generated by microsurgical methods (Pelletier *et al.*, 2000). This led to the observation that no Golgi can re-form in cytoplast containing only peripheral ER. However, this method is a cell by cell approach, assumes that no Golgi exist in the cell periphery, and above all is technically demanding and has so far only been mastered by one team (Pelletier *et al.*, 2000; Sheff *et al.*, 2002).

Here we develop a new method that allows one to enzymatically inactivate the Golgi apparatus in intact living cells. We took advantage of two sets of studies, both centered on the use of horseradish peroxidase (HRP). On the one hand, HRP has been used to inactivate the function of endosomes (Futter *et al.*, 1996; Brachet *et al.*, 1999; Pond and Watts, 1999). In these studies, endosomes are filled with HRP, alone or fused to transferrin or to EGF, and treated with 3,3′-diaminobenzidine (DAB) in the presence of a low concentration of H_2O_2. HRP-dependent polymerization of DAB cross-links the target organelle and blocks its dynamics. This treatment is specific for organelles loaded with HRP, here the endosomes, and does not affect the function of other organelles like the Golgi (Brachet *et al.*, 1999). On the other hand, the work of Cutler, Hopkins, and coworkers showed that active HRP can be expressed in the lumen of secretory compartments and, when fused to the transmembrane domain of the *trans*-Golgi/TGN enzyme sialytransferase, HRP can be stably expressed in the lumen of Golgi cisternae (Connolly *et al.*, 1994; Stinchcombe *et al.*, 1995).

We devised ways to apply HRP-based organelle cross-link to the Golgi apparatus and analyze whether it allows specific and drug-free inactivation of Golgi dynamics and function, providing a unique set-up to study Golgi maintenance in interphase cells.

MATERIALS AND METHODS

Chemicals and Antibodies

Culture medium, penicillin/streptomycin, and sodium pyruvate were obtained from Invitrogen (Carlsbad, CA) and Geneticin was from Invitrogen. Paraformaldehyde was purchased from Carlo Erba (Valencia, CA). Nocodazole (suspended as a stock of 10 mM in dimethyl sulfoxide [DMSO]), DAB tablets, stabilized H_2O_2 30% were all obtained from Sigma. For cross-linking experiments, Sigma Fast DAB tablets were diluted three times more than advised by the provider. Brefeldin A (BFA) was obtained from Epicenter Technologies (Madison, WI) and suspended as a stock solution of 5 mg/ml in methanol. Endoglycosidase H (EndoH) was purchased at New England Biolabs (Beverly, MA). Alexa Fluor633-transferrin and Alexa Fluor–labeled secondary antibodies were obtained from Molecular Probes (Eugene, OR), and Cy3- and Cy5-labeled secondary antibodies were obtained from Jackson ImmunoResearch Laboratories (West Grove, PA). Anti-giantin (TA10) was a previously described single chain antibody (Nizak *et al.*, 2003), anti-GMAP210 was kindly provided by Dr. M. Bornens (Institut Curie, Paris, France), anti-GM130 was from BD Biosciences (San Jose, CA), and anti-TGN46 was from Serotec (Raleigh, NC).

Plasmid Constructs

pManII-HRP was constructed by replacing the AgeI/NotI enhanced GFP (EGFP) insert from pManII-EGFP plasmid (kind gift from J. White, EMBL, Germany) by the HRP coding sequence. HRP was amplified by PCR using the following primers: 5′ CGCGGATCCACCGGTCGCCACC ATG CAG TTA ACC CCT ACA TTC 3′ and 5′ TACCTAGGTGCGGCCGCTTAAGAGTTGCTGTTGACCAC 3′, cut with AgeI and NotI and inserted in the target plasmids opened similarly.

Cell Culture

HeLa cells were grown in DMEM containing 4.5 g/l glucose supplemented with 10% fetal calf serum, penicillin-streptomycin, and sodium pyruvate in a 5% humidified CO_2 incubator. Transfection was achieved using the calcium phosphate precipitate method described in Jordan *et al.* (1996). Stable cell lines expressing mannosidase II (ManII)-HRP were obtained after selection using 400 μg/ml geneticin.

For transferrin uptake, 5 μg/ml Alexa633-labeled transferrin was added in the culture medium at the same time as BFA, and cells were incubated for 90 min at 37°C.

Golgi cross-linking was achieved essentially as described in Brachet *et al.* (1999) for endosome cross-linking after HRP internalization. Cells expressing or not HRP in Golgi cisternae were washed in PBS and incubated with DAB + 0.003% H_2O_2 for 30 min at 0°C. Cells were then washed and fixed or further incubated in normal medium before fixation.

Electron Microscopy

Epon Embedding. DAB labeling was either done on living cells as described above or on fixed cells as previously (Nizak *et al.*, 2004) using DAB (0.25 mg/ml, Sigma) and 0.003% H_2O_2 (Sigma) in phosphate-buffered solution for 40 min. Cells were then fixed in 4% paraformaldehyde and 0.5% glutaraldehyde for 4 h at room temperature, rinsed, and postfixed 1 h at room temperature in reduced osmium (1:1 mixture of 2% aqueous potassium ferrocyanide) as described previously by Karnovsky (1971).

After postfixation the cells were embedded in agar 2%, dehydrated in ethanol, and processed for Epon embedding. Thin sections were cut on a Reichter-E ultramicrotome (Reichter-Jung, Vienna, Austria), collected on copper grids and stained with lead citrate for 2 min. Sections were then examined with a CM 10 Philips electron microscope (FEI, Eindoven, The Netherlands) at 80 kV.

Immunogold Labeling. Transfected HeLa cells were incubated with DAB + H_2O_2 on ice for 30 min and fixed with 2% (wt/vol) paraformaldehyde with 0.2% (wt/vol) glutaraldehyde, in 0.1 M phosphate buffer, pH 7.4. Cell pellets were processed for ultracryomicrotomy as previously described (Raposo *et al.*, 1997). Ultrathin cryosections were prepared with an ultracryomicrotome Ultracut FCS (Leica, Vienna, Austria) and immunogold labeled with the indicated primary antibodies and using protein A conjugated to 10-nm gold (Cell Microscopy Center, AZU, Utrecht, The Netherlands). Sections were analyzed under a Philips CM120 electron microscope, and digital acquisitions were made with a numeric camera Keen View (Soft Imaging Systems, Münster, Germany).

Photoconversion

ManII-HRP cells were transfected with a plasmid controlling the expression of Dendra2-GM130 (Evrogen, Moscow, Russia). Twenty-four hours later, cells were observed alive in complete medium using a Ludin chamber placed on a LSM510-confocal microscope and imaged sequentially using green and red fluorescence settings. Cells were treated with DAB/H_2O_2 for 30 min on ice, washed, warmed-up in complete medium at 37°C, and imaged in green and red channels. Dendra2-GM130 located on the Golgi apparatus were then specifically photoconverted using a 405-nm laser beam scanning in a region of interest to avoid photoconversion of the cytoplasmic form of GM130. Cells were imaged just after the photoconversion and 90 min later. A transmitted light image was also acquired to localize the cross-linked, DAB-positive Golgi apparatus.

Vesicular Stomatitis Virus G Protein Trafficking

Cells were transfected with a plasmid allowing the expression of GFP-VSVG^{ts045} and incubated overnight at 40°C. Transport to the Golgi complex and to the plasma membrane was initiated by shifting cells at 32°C. In certain experiments, cells were cooled down at 0°C and cross-linked using DAB/

H_2O_2 before shifting at 32°C. Expression at the plasma membrane was quantified using the VG antibody, directed against the exoplasmic domain of vesicular stomatitis virus G (VSV-G) protein, in the absence of detergent. After incubating the cells with a fluorescent anti-mouse antibody, when necessary cells were rapidly fixed again using paraformaldehyde, permeabilized, and counterstained using another antibody. For fluorescence-activated cell sorting (FACS) analysis, cells were first trypsinized before being fixed and stained. For quantification of Golgi arrival, sensitivity of VSV-G glycosylation to EndoH, cells expressing GFP-VSV-G^{ts045} blocked in the ER overnight at 40°C were pulse labeled using 150 μCi/ml [^{35}S]TransLabel (ICN Biomedicals), washed in radioactive-free medium, cross-linked or not, and incubated at 32°C. Cells were then lysed in immunoprecipitation (IP) buffer (150 mM NaCl, 20 mM Tris, pH 7.5, 5 mM EDTA, 1% Triton X-100, and 0.20% bovine serum albumin [BSA]), and GFP-VSVG was precipitated using monoclonal anti-GFP, and treated or not with EndoH following the instructions of the provider, and radioactive proteins were separated by SDS-PAGE and quantitatively imaged using a PhosphorImager (GE Healthcare, Waukesha, WI).

Fluorescence Microscopy

Cells were stained using Alexa488-labeled (Molecular Probes) or Cye-dye–labeled secondary antibodies (Jackson ImmunoResearch). Alternatively the natural fluorescence of GFP and Dendra2 was used. Optical microscope used in this study were as follows: 1) Leica DMRA (Wetzlar, Germany) equipped with a Micromax cooled CCD camera controlled by the Metamorph software (Molecular Devices, Berkshire, United Kingdom). Images were acquired using the 63× NA 1.32 oil ph3 CS (HCX PL APO) objective, and fluorescence filters A4, L5, Y3, and Y5 from Leica; and 2) Zeiss LSM510 meta installed with a 405-nm laser diode and argon and helium laser (Thornwood, NY). The objective used for imaging was the 63× NA 1.4 oil differential interference contrast (DIC; Plan Apochromat) together with the fluorescein isothiocyanate (FITC) and Rhod filters.

Deconvolution and Three-dimensional Image Processing

Cells fluorescently labeled were examined under a classical upright motorized microscope (Leica DMRA2). Images were acquired using an oil-immersion objective (×100 PL APO HCX, 1.4 NA) mounted on a piezo-electric motor (LVDT, Physik Instruments, Waldbronn, Germany) and a high-sensitive cooled interlined CCD camera (Roper CoolSnap HQ, Tucson, AZ). The system was controlled by the Metamorph Software (Molecular Devices). Deconvolutions were performed on stacks of images taken with a 0.3-μm plane-to-plane distance, using the three-dimensional (3D) deconvolution module of Metamorph and the fast iterative constrained Point Spread Function-based algorithm. Surface rendering and volume quantifications were performed using Amira software (TGS, San Diego, CA).

RESULTS

Expression of HRP in the Golgi Complex and Precipitation of DAB in the Lumen of Golgi Cisternae in Living Cells

In initial attempts to in vivo cross-link Golgi cisternae, we found that the ST-HRP constructed by Connolly *et al.* (1994), although usable, also stained post-Golgi elements after DAB treatment. We thus constructed Golgi-targeted HRP-fusion proteins by fusing HRP to the transmembrane domains of different Golgi enzymes. This strategy has been successfully used before to target GFP to specific Golgi subcompartments (Storrie *et al.*, 1998). We removed the enhanced GFP (EGFP) from pManII-EGFP and replaced it with HRP (see *Materials and Methods*). Immunofluorescence experiments showed that, as its fluorescent counterpart, ManII-HRP stably expressed in HeLa cells and stained using an anti-HRP antibody was colocalized with Golgi markers like GM130 or TGN46 (Figure 1A). The experiments that we report here were done using a stable ManII-HRP HeLa clone. We further confirmed that, similar to ST-HRP (Connolly *et al.*, 1994), these fusion proteins allow efficient targeting of active HRP to Golgi cisternae. Golgi localized HRP activity was revealed on fixed cells by DAB/H_2O_2, and the DAB precipitate colocalized with *cis* to *trans*-Golgi markers like GM130 and TGN46.

We then asked whether DAB precipitation could also occur in living cells. We used the protocol developed previously by Brachet *et al.* (1999) to achieve ablation of early endosomes after endocytosis of transferrin-HRP, because very little nonspecific effects of DAB/H_2O_2 were observed in their conditions. HeLa ManII-HRP were thus treated with diluted DAB in the presence of a low concentration of H_2O_2 for 30 min on ice. Similar results were obtained after 15 min at room temperature. This treatment led to the formation of a brown precipitate in the region of the Golgi. Immunofluorescence experiments using different Golgi markers like GM130 and TGN46 (Figure 1B, a–c) confirmed that this precipitate indeed stained the Golgi complex. No such precipitate was observed after treatment of living control HeLa cells (Figure 1B, d and e). We noticed that antibody staining of certain luminal markers, such as endogenous galT or exogenous ManII-HRP, is strongly reduced after DAB/H_2O_2 treatment as if antigen accessibility was compromised due to DAB precipitation. This possibility was further suggested by the fact that the signal corresponding to fluorescent proteins like EGFP-galT was not affected to the same extent. We further confirmed that the DAB precipitate was specifically formed in the lumen of Golgi cisternae by electron microscopy (EM). ManII-HRP cells were fixed and incubated with DAB/H_2O_2 before being processed for EM. The DAB precipitate was deposited in either the medial and *trans* cisternae, or in all Golgi cisternae, probably depending on the expression level (Figure 2A). No staining was detected in the ER or in wild-type HeLa cells (Figure 2C). Importantly, a Golgi staining was also observed in cells incubated before fixation with DAB/H_2O_2 (Figure 2B), indicating that the DAB precipitate is specifically formed in the lumen of Golgi cisternae in living cells.

This shows that expression of HRP in the lumen of a compartment can drive the formation of DAB precipitate, opening the possibility of specific organelle inactivation in a more generally applicable way than previously described methods based on HRP uptake.

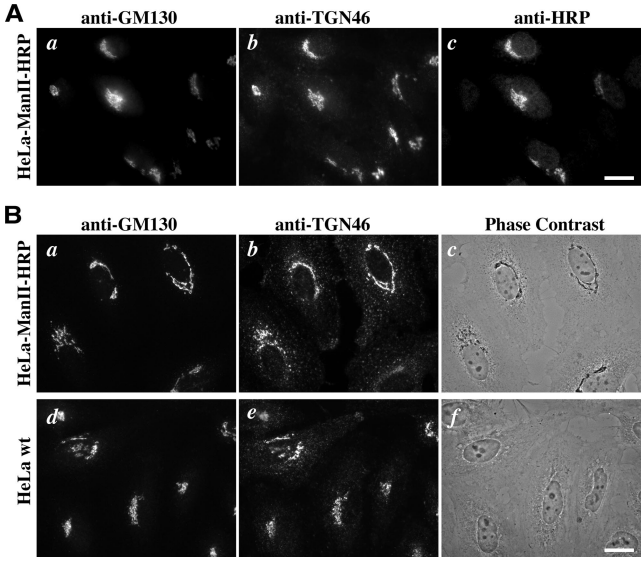

Figure 1. DAB precipitation in living cells by Golgi localized HRP. (A) HeLa cells stably expressing ManII-HRP were fixed and stained for GM130 (a), TGN46 (b), and HRP (c). Extensive colocalization of ManII-HRP with Golgi markers was observed. Bar, 20 μm. (B) HeLa cells stably expressing ManII-HRP (a–c) or wild-type Hela cells (d–f) were incubated in DAB/H_2O_2 alive (see *Materials and Methods*) and then fixed and stained for GM130 (a and d) and TGN46 (b and e). This experiment shows that specific DAB precipitation (see the phase-contrast image in c and f) can be achieved in living HeLa ManII-HRP cells. Bar, 20 μm.

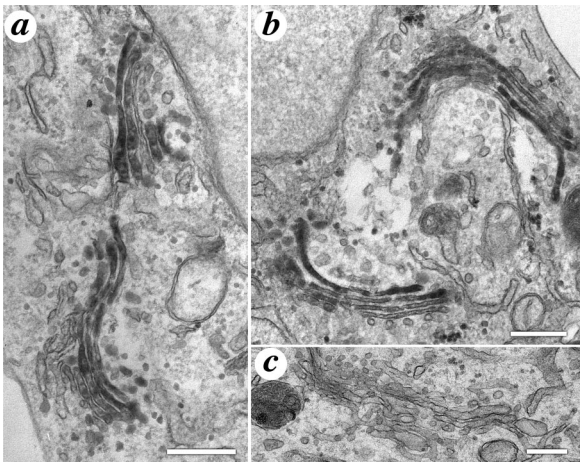

Figure 2. Specific DAB deposition in Golgi cisternae after DAB incubation of fixed or living ManII-HRP–expressing HeLa cells. HeLa ManII-HRP cells were either fixed and stained with DAB/H_2O_2 (a) or incubated alive with DAB/H_2O_2 and then fixed (b) before being processed for EM. As a control (c), wild-type HeLa cells were treated as in a. Note that the DAB precipitate was similarly restricted to Golgi cisternae in cells stained fixed or alive. Bar, 250 nm.

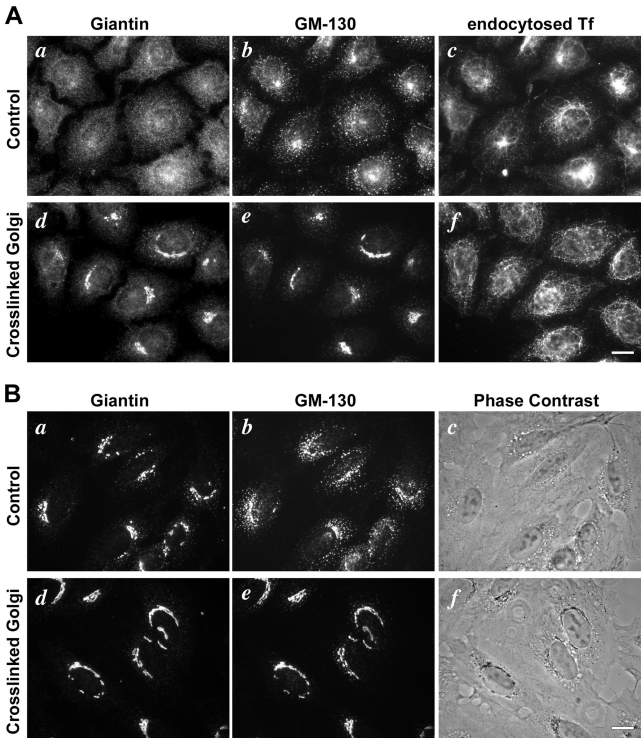

Figure 3. Golgi-localized DAB precipitation inactivates Golgi dynamics. (A) HeLa ManII-HRP cells were incubated with H_2O_2 alone (a–c) or with DAB/H_2O_2 (d–f) before being treated with brefeldin A (BFA) for 90 min. Cells were fed with fluorescent transferrin during the BFA treatment (see c and f). Cells were then fixed and stained using anti-giantin (a and d) and anti-GM130 (b and e) antibodies. Although BFA is normally active in cells treated with DAB/H_2O_2 and although endocytosis still proceeds in these cells (see the fluorescent tubular endosomes in f), DAB precipitation in Golgi cisternae prevents massive giantin relocation to the ER and GM130 transportation back to the intermediate compartment after BFA treatment, indicating that Golgi dynamics is strongly perturbed. (B) HeLa ManII-HRP cells were treated with H_2O_2 alone (a–c) or with DAB/H_2O_2 (d–f), incubated on ice 60 min, and warmed up in nocodazole for 90 min. Cells were then fixed and stained for giantin (a and d) and GM130 (b and e). The corresponding phase-contrast image is also shown in c and f. Although efficient Golgi dispersion was induced in control cells, cross-linked Golgi complexes (see the contrast phase image in f) were largely resistant to microtubule depolymerization, further highlighting inactivation of Golgi dynamics. Bar, 20 μm.

Perturbation of Golgi Dynamics after Cross-Linking

According to the endosome ablation studies and because the DAB precipitate was only found inside the Golgi cisternae, it was likely that DAB/H_2O_2 treatment would lead to the specific cross-linking and hence inactivation of the Golgi complex. We tested this hypothesis by evaluating the sensitivity of organelles in cross-linked cells to particular drug treatments. ManII-HRP cells were incubated or not with DAB/H_2O_2 before being treated by BFA. BFA addition leads to the rapid relocation of Golgi markers such as Golgi enzymes or giantin to the ER, whereas others like GM130 or GMAP210 are transported into the intermediate compartment, mixed with the endosomes (e.g., TGN46), or released to the cytosol (e.g., COPI). This illustrates the extreme dynamics that underlies steady-state Golgi localization. In nontreated cells (Figure 3A, a–c), we confirmed that BFA treatment induces the relocation of giantin to the ER, whereas GM130 is transported to the intermediate compartment. Addition of BFA also induces a strong tubulation of early endosomes, as observed by fluorescent transferrin endocytosis (Figure 3A c). In contrast, after Golgi cross-linking (Figure 3A, d–f), ManII-HRP cells did not react to BFA by relocating Golgi markers. Careful examination revealed only weak GM130 in the cell periphery after BFA treatment but the majority of GM130 and giantin staining stays associated to the DAB-positive Golgi. One possibility was that DAB/H_2O_2 incubation of ManII-HRP cells was toxic, inactivating nonspecifically membrane dynamics, or that BFA sensitivity was lost after DAB/H_2O_2 treatment. In cross-linked cells, however, early endosomes still became tubular and continued to efficiently uptake fluorescent transferrin (Figure 3Af). Thus, cross-linked cells are still alive and dynamic and BFA is still active in these cells. This experiment confirms that, as shown before (Futter *et al.*, 1996; Brachet *et al.*, 1999; Pond and Watts, 1999), DAB/H_2O_2 treatment did not generally affect the cells and indicates that the Golgi complex is no longer dynamic after DAB/H_2O_2-based cross-linking.

Another way to illustrate the extreme dynamics of Golgi structure is to perturb the function of the microtubule network. For example, depolymerizing interphasic microtubules with nocodazole results in the dispersion of the Golgi complex in the form of mini-stacks located throughout the cytoplasm (Cole *et al.*, 1996; Storrie *et al.*, 1998). Because this dispersion is strongly dependent on an active Golgi-to-ER pathway (Storrie *et al.*, 1998), we tested whether cross-linked Golgi still dispersed in the presence of nocodazole. Non-DAB/H_2O_2–treated ManII-HRP cells reacted normally to nocodazole addition, and a dispersed Golgi was observed after a 90-min treatment at 37°C as imaged by anti-GM130 and giantin antibodies (Figure 3B, a and b). In contrast, very little Golgi dispersion was observed after nocodazole addition in ManII-HRP cells pretreated with DAB/H_2O_2 (Figure 3B, d–f). In these cells, the shape of giantin- and GM130-positive Golgi membranes was almost unaffected by nocodazole treatment, and these membranes stayed colocalized with the DAB precipitate. This further indicated that DAB precipitation inactivates Golgi dynamics.

In Vivo Cross-Linking of ManII-HRP–positive Compartment Leads to Golgi Function Inactivation

We next tested whether incubation of ManII-HRP cells with DAB/H_2O_2 led to inactivation of the Golgi apparatus function. Secretion was quantified using the ts045 mutant of the VSV-G protein. This protein remains in the ER at restrictive temperature (40°C) and only folds properly, trimerizes, and exits the ER at permissive temperature (32°C). At early time points, the VSV-G protein transits through the Golgi complex (30 min), where its glycosylation becomes Endo H–resistant and reaches the plasma membrane later on (after 45–60 min). The use of the VG mAb directed against the exoplasmic domain of VSV-G allows one to quantify, using nonpermeabilized cells, the extent of cell surface expression. The total amount of VSV-G is either visualized using the monoclonal P5D4 (when using viral infection) or the fluorescence of the recombinant VSVG-EGFP fusion molecule.

We first analyzed VSV-G trafficking by immunofluorescence and microscopic observation (Figure 4A). Control HeLa ManII-HRP cells treated only with H_2O_2 secreted

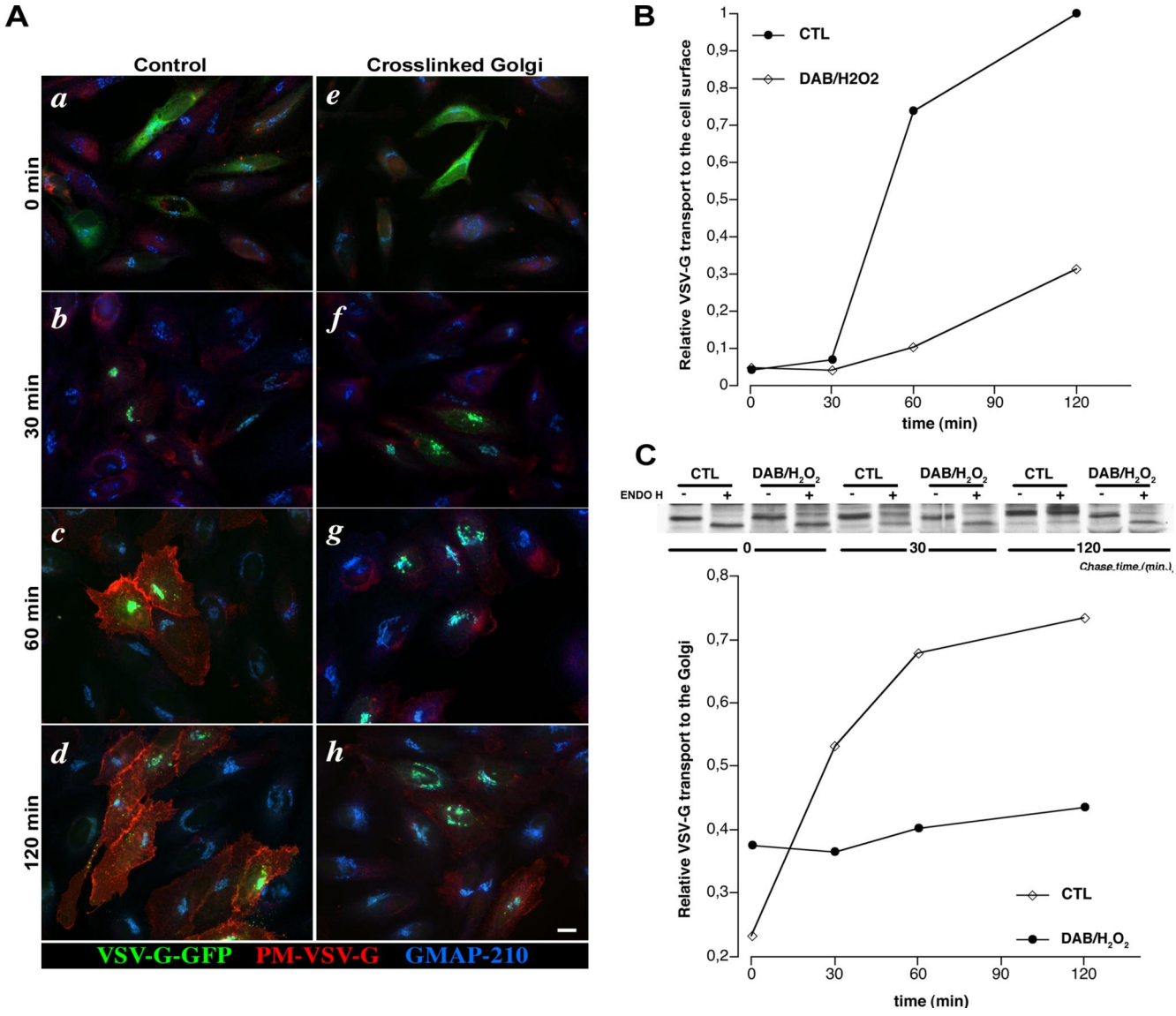

Figure 4. Golgi-localized DAB precipitation inactivates VSV-G secretion. (A) HeLa-ManII-HRP cells were transfected with GFP-VSV-G^{ts045} encoding plasmids and incubated overnight at 40°C. Cells were then shifted to 32°C without (a–d) or with (e–h) pre-treatment with DAB/H_2O_2 and fixed in paraformaldehyde. Cells were processed for immunofluorescence (see *Materials and Methods*) to stain plasma membrane–localized VSV-G proteins (in red) and the Golgi complexes (in blue), whereas the bulk of GFP-VSV-G protein is directly visible in green. As expected, in the absence of Golgi cross-linking, GFP-VSV-G^{ts045} is found in the ER just before shifting at permissive temperature (a) and then reaches the Golgi apparatus (b) before being expressed at the plasma membrane (c and d). In contrast, after cross-linking the Golgi with DAB/H_2O_2, GFP-VSV-G^{ts045} exits the ER at permissive temperature and reaches the Golgi region (e and f) but is barely visible at the plasma membrane even after 120 min (h). Bar, 20 μm. (B) An experiment similar to the one described in A was analyzed by FACS to quantify the arrival of VSV-G^{ts045} at the plasma membrane. As observed in A, whereas in nontreated cells VSV-G is efficiently transported at the plasma membrane, cross-linking of the Golgi strongly reduces its transport to the plasma membrane. (C) A similar experiment was carried out but using pulse chase and immunoprecipitation of VSVG-GFP proteins followed by de-glycosylation, SDS-PAGE separation, and PhosphorImager-based quantification. VSV-G is blocked in a pre-Golgi compartment in cross-linked cells, as indicated by the persistence of EndoH sensitivity of its glycosylation.

VSV-G with normal kinetics: it was accumulated in the ER at 0 min and then was transported toward the Golgi apparatus (30 min) before being expressed at the plasma membrane (Figure 4A, a–d). In contrast, only low plasma membrane staining was observed in HeLa ManII-HRP treated with DAB/H_2O_2 (Figure 4A, e–h), indicating a strong decrease in protein VSV-G secretion after cross-linking. This block was quantified by FACS analysis (Figure 4B).

Interestingly, the VSV-G exited normally the ER, although with somewhat slower kinetics, and was targeted toward the cross-linked Golgi area. As suggested before (Figure 3), this further indicates that the cross-linking is not generally inactivating cell dynamics and that intracellular trafficking is not globally affected. Careful examination revealed that the VSV-G–positive structures were not colocalized but were juxtaposed to cross-linked Golgi elements (see below),

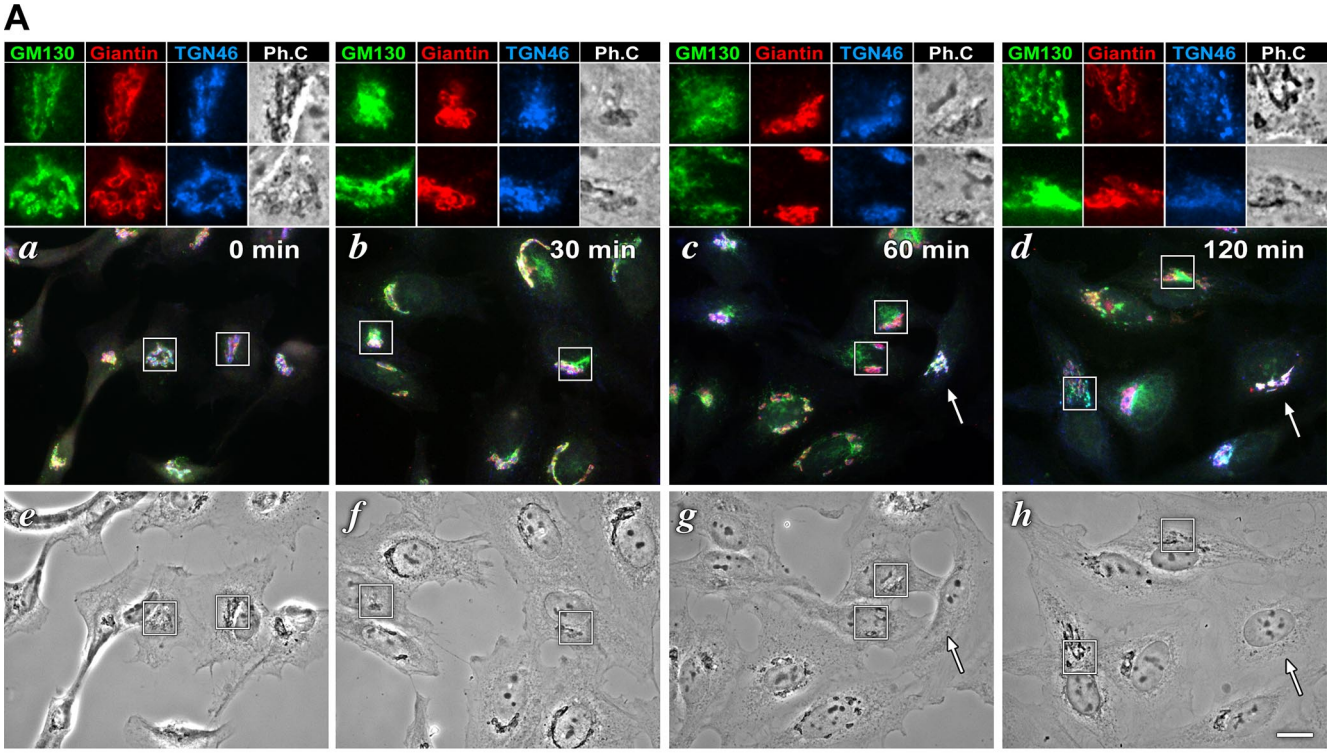

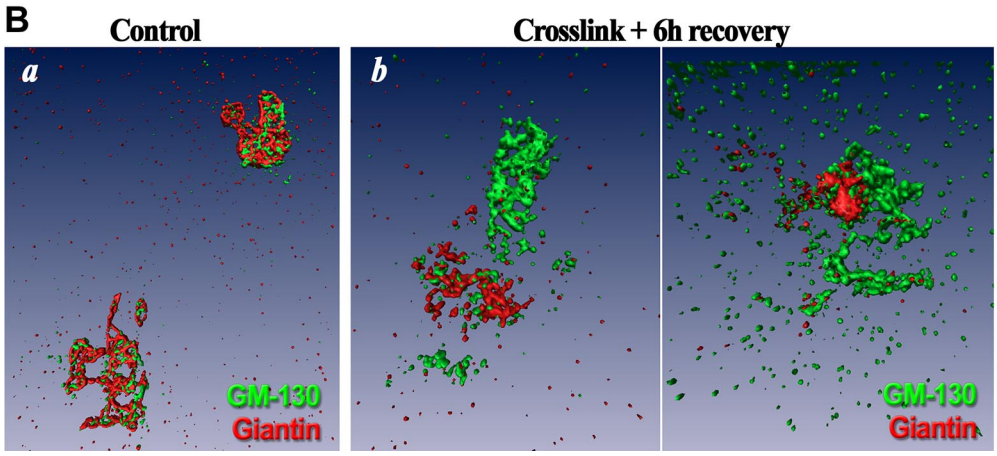

Figure 5. Formation of a new Golgi-like structure in cross-linked cells. (A) HeLa ManII-HRP were treated with DAB/H_2O_2, washed, and then fixed (a and e) or incubated in normal medium at 37°C for 30 min (b and f), 60 min (c and g), or 120 min (d and h) before being fixed. Cells were then stained using anti-GM130 (green), anti-giantin (red), and anti-TGN46 antibodies (blue). The areas boxed in a–d are shown enlarged on the top. Although the three Golgi markers were expressed in closely apposed structures, co-stained by DAB, just after Golgi cross-linking, GM130 rapidly labels a separate compartment, also stained by TGN46 at later time points (120 min) but not by giantin, which stays colocalized with the DAB-positive structure (seen in e–h). Note that extensive colocalization between these Golgi markers was kept in cells that did not display DAB precipitation (arrows). This suggests that a Golgi-like structure, only partially positive for Golgi markers, forms in cells after Golgi inactivation. Bar, 20 μm. (B) ManII-HRP HeLa cells kept in normal medium (a) or cross-linked using DAB/H_2O_2 and let to recover for 6 h at 37°C in normal medium were fixed and stained by immunofluorescence using anti-GM130 (red) and anti-giantin (green) antibodies. Preparations were then analyzed by 3D-deconvolution and surface rendering. Although GM130 and giantin (a) juxtaposed on the same structures in control cells, they localized on different structures after Golgi cross-linking and recovery.

which prompted us to test whether the VSV-G was blocked in an early pre-Golgi compartment. Analysis of VSV-G glycosylation after shifting to permissive temperature indeed revealed that, in contrast to control conditions, VSV-G did not acquire EndoH-resistant glycosylation (Figure 4C).

Golgi Complex Rebuilding after Inactivation

The in vivo cross-linking of ManII-HRP leads to ablation of Golgi function. A key question is whether a new Golgi apparatus can re-form after inactivation or whether the cell needs a pre-existing Golgi structure to build a new Golgi. We thus studied Golgi recovery after cross-linking, following the behavior of several Golgi markers: transmembrane proteins located in the *cis*- and medial Golgi (giantin) and in the *trans*/TGN (TGN46) as well as peripheral proteins (GM130). As expected, immunofluorescence staining of treated cells showed that just after Golgi inactivation (Figure 5A, a and e), these three proteins were detected in largely overlapping Golgi stained by DAB. As soon as 30 min after the cross-link, GM130 was detected on new structures, often found apposed to the "old" inactivated Golgi, whereas the two transmembrane proteins, giantin and TGN46, were still located only on DAB-positive Golgi elements (Figure 5A, b and f). At later time points, more GM130 was detected on these new structures and was progressively lost by the old inactivated ones. The proportion of TGN46 detected on the GM130-positive new structures also increased but to a lesser extent (Figure 5A, c and d). In contrast, giantin did not partition at all on these elements and was still found located on the inactivated Golgi. 3D reconstruction after deconvolution confirmed that, whereas in control cells GM130 and giantin are closely apposed on Golgi structures (Figure 5Ba), after cross-linking they partition on two separate structures (Figure 5Bb).

More generally, we analyzed the behavior of a large set of Golgi markers (Table 1) and observed that the vast majority of these markers was found on the newly formed, GM130-positive, structure with the notable exception, in addition to giantin, of the medial marker CTR433 (Jasmin *et al.*, 1989) and the Golgi v-SNARE GS15 (Xu *et al.*, 1997, 2002). Surprisingly, although GS15 was not found on newly formed Golgi-like elements, its partners YKT6, GS18, and syntaxin-5 (Xu *et al.*, 2002) were localized on these new structures. Note also that the Golgi enzyme galactosyl transferase was absent from re-formed structures.

We observed that GM130 localization on this new structure still occurred in the presence of cycloheximide and thus did not rely on new protein synthesis. However, it was unclear whether these Golgi-like elements were completely built de novo or whether components were recycled from the old inactivated Golgi stacks to the newly formed structure. In particular, GM130 that quickly labeled Golgi-like structures, could either come from the old cross-linked Golgi membranes or from a cytosolic pool (Yoshimura *et al.*, 2001). To answer to this question, we set up a photo-conversion experiment that allows to distinguish GM130 molecules localized on the inactivated Golgi stacks from cytosolic GM130. We used a photoconvertible version of GM130 fused to Dendra2 (Gurskaya *et al.*, 2006) and confirmed that it normally targets the Golgi apparatus (unpublished data). ManII-HRP cells expressing Dendra2-GM130 were cross-linked and observed by confocal microscopy (Figure 6, left panel). Dendra2-GM130 proteins localized on the inactivated Golgi membranes were then irreversibly identified: a region of interest was drawn around the cross-linked Golgi apparatus, and Dendra2-GM130 was then photoconverted to red only inside this region (Figure 6, middle panel). The same cells were imaged again 90 min later (Figure 6, right panel), and we observed that the photoconverted GM130 was also found on the re-formed Golgi-like structure, indicating that a fraction of GM130 was relocated from the inactivated Golgi to the new structure.

EM observation suggested that, although they are positive for a large number of Golgi markers, these new elements may not be fully formed and mature Golgi structures. Time course studies indeed did not reveal any newly formed Golgi stacks after inactivation (Figure 7). Rather, we observed that cross-linked old Golgi membranes persist in the cells after DAB treatment in the form of long cisternae that slowly dissociates from each other. Four hours after cross-linking, DAB-positive independent cisternae were clearly observed, as if a glue attaching cisternae to each other to build a stack had been lost. Importantly, in the vicinity of the cross-linked element, only tubulo-vesicular elements were observed that were either dispersed or, more rarely, clustered (see the outlined zone in Figure 7d) and that are likely to be the newly formed structures observed by immunofluorescence. Immunoelectron microscopy (Figure 8) indeed revealed that the bulk of GM130 was not localized anymore on cross-linked Golgi elements as observed on control cells (Figure 8B) but rather juxtaposed to these inactivated cisternae, in cytoplasmic domains where no Golgi stacks can be detected (Figure 8A), confirming the results obtained using light microscopy and deconvolution. In some case, large vacuolar structure apposed to inactivated Golgi elements were positive for GM130 (Figure 8A).

These observations suggested that new structures, positive for both *cis*- and *trans*- TGN Golgi markers but not morphologically similar to Golgi elements form rapidly after cross-linking. Because we observed that although post-Golgi secretion was blocked after Golgi inactivation, cargo left the ER and were transported toward the inactivated Golgi after

Table 1. Localization of Golgi markers 120 min after DAB/H_2O_2-based inactivation of Golgi complexes in ManII-HRP Hela cells

Marker	Localization after 120 min
Giantin	Cross-linked Golgi
CTR433	Cross-linked Golgi
GS15	Cross-linked Golgi
β-COP	New Golgi-like structure
GMAP210	New Golgi-like structure
GM130	New Golgi-like structure
GCC88[a]	New Golgi-like structure
GCC97[a]	New Golgi-like structure
GCC185[a]	New Golgi-like structure
GRASP55[a]	New Golgi-like structure
GRASP65	New Golgi-like structure
GS28	New Golgi-like structure
p115	New Golgi-like structure
p230	New Golgi-like structure
rab6	New Golgi-like structure
Syntaxin-5	New Golgi-like structure
TGN46	New Golgi-like structure
VSV-G	New Golgi-like structure
YKT6	New Golgi-like structure
galT	Absent[b]

[a]These markers were tested using GFP-tagged expressed proteins.

[b]The DAB precipitates in the lumen of the cisternae prevents immunodetection of endogenous galT. When using GFP-galT, a signal can be visualized in the cross-linked Golgi.

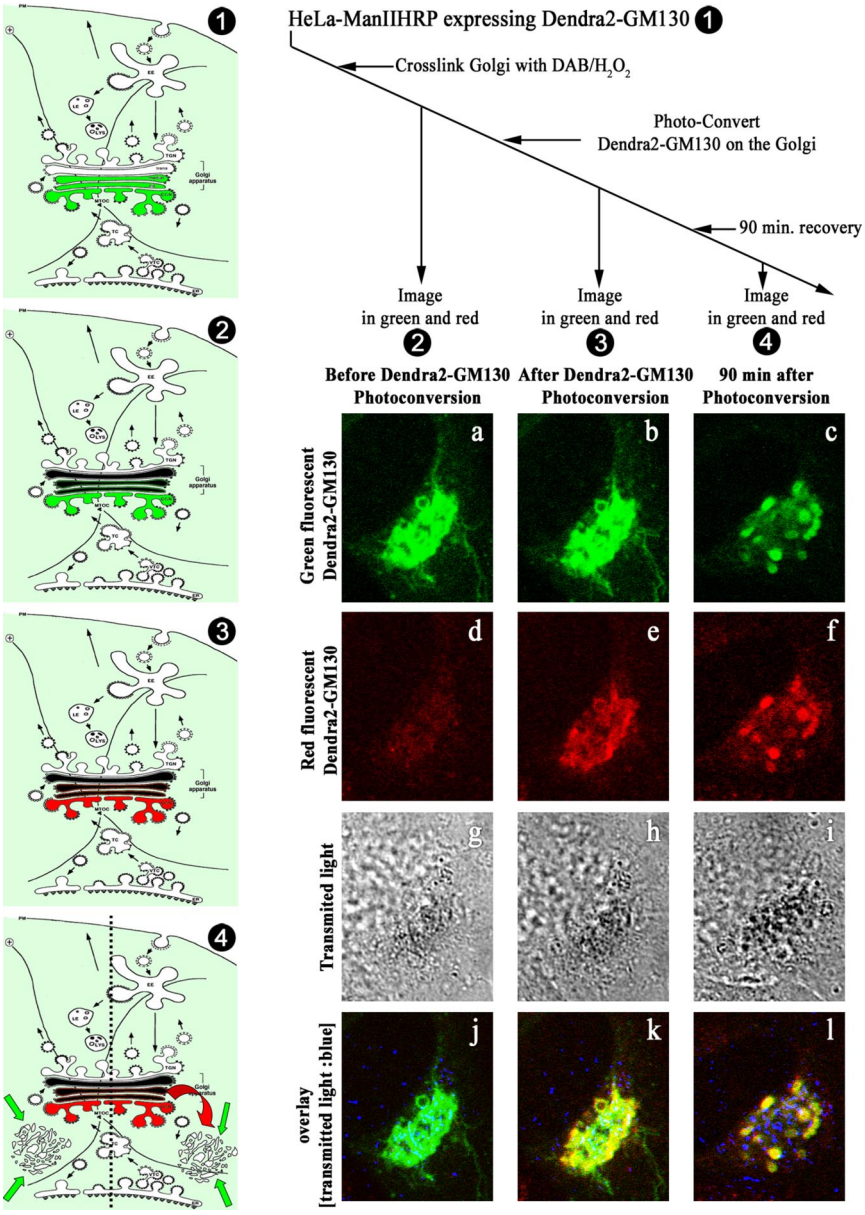

Figure 6. Recycling of GM130 from the old, inactivated Golgi to the new Golgi-like structure. HeLa ManII-HRP were transfected 24 h before the experiment to express GM130 tagged with a green-to-red photoconvertible fluorescent protein, Dendra2. The scheme of the experiment is depicted in the left panel. Cells expressing green fluorescent GM130 (1) were cross-linked using DAB/H_2O_2 (2) and imaged using a LSM510 confocal microscope in the green (a) and red (d) channels. A transmitted light image was also acquired to identify cross-linked elements (g). The bottom panels shows an overlay where the transmitted light image has been pseudocolored in blue. Golgi localized GM130 molecules were then photoconverted using a 405-nm beam illumination in a region of interest outlining specifically Golgi elements (3). Green, red, and transmitted light images were acquired (b, e, and h, respectively), showing that photoconverted GM130 are localized on the inactivated Golgi. Cells were then let to recover for 90 min at 37°C and imaged again (c, f, and i). Fluorescent structures, not colocalized with inactivated membranes (see the juxtaposed blue and green signal in panel l) were identified. These structure are fluorescent both in green and red, showing that at least a fraction of GM130 has recycled from the old, inactivated Golgi to the newly formed structure.

cross-linking (Figure 4A, f–h), we asked whether these cargo were accumulated in the newly formed structures. VSV-G^{tsO45} was thus blocked in the ER at the nonpermissive temperature, the Golgi was inactivated by DAB treatment, and cells then were shifted to permissive temperature for 1 h, fixed, and analyzed by immunofluorescence (Figure 9). In control conditions, VSV-G molecules were expressed at the plasma membrane and in Golgi elements positive for both GM130 and giantin. In contrast, after Golgi inactivation, VSV-G molecules were accumulated in structures positive for GM130 but negative for giantin and hence likely to be the newly formed Golgi-like elements.

Altogether, this indicates that new Golgi-like elements are formed after Golgi inactivation. They are positive for most, but not all, Golgi markers, they contain newly synthesized secretory cargo but do not display a normal Golgi shape, and they are incompetent for transporting the cargo toward the plasma membrane. These observations suggest that a functional Golgi apparatus is necessary to rebuild rapidly a new functional and morphologically normal Golgi apparatus.

DISCUSSION

HRP-based organelle inactivation was shown to be a powerful tool to study the role of a particular organelle in a trafficking route (see Futter *et al.*, 1996; Brachet *et al.*, 1999; Pond and Watts, 1999; Ang *et al.*, 2004). However, it has so far relied on HRP-labeled probes captured from the extracellular medium and has thus been applicable only to organelles connected to the endocytic pathway. Here we show that this strategy can be extended to virtually any organelle if at least one specific marker is known that can be fused to HRP in its luminal domain. HRP must be expressed in the lumen of the compartment both to protect it from the reducing environment of the cytosol and to restrict the precipitation to the targeted organelle, which is essential to ensure

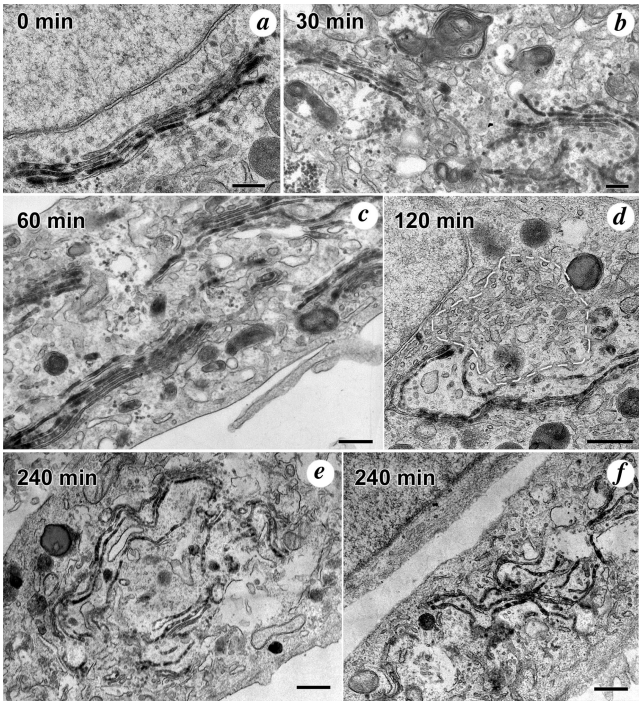

Figure 7. EM observation of cells after Golgi cross-linking. HeLa ManII-HRP were treated as in Figure 4 and processed for EM 0 min (a), 30 min (b), 60 min (c), 120 min (d), or 240 min (e and f) after DAB/H_2O_2 treatment. No DAB-negative stacks of cisternae were observed in cells visibly cross-linked, even 2 h after DAB treatment. Only tubulovesicular clusters (region outlined in d) were sometimes observed close to cross-linked Golgi. Note that cross-linked cisternae, closely apposed at t = 0 min (a), detached from each other after the cross-link and were found as independent long cisternae 120 min after cross-linking (d–f). Bar, 250 nm.

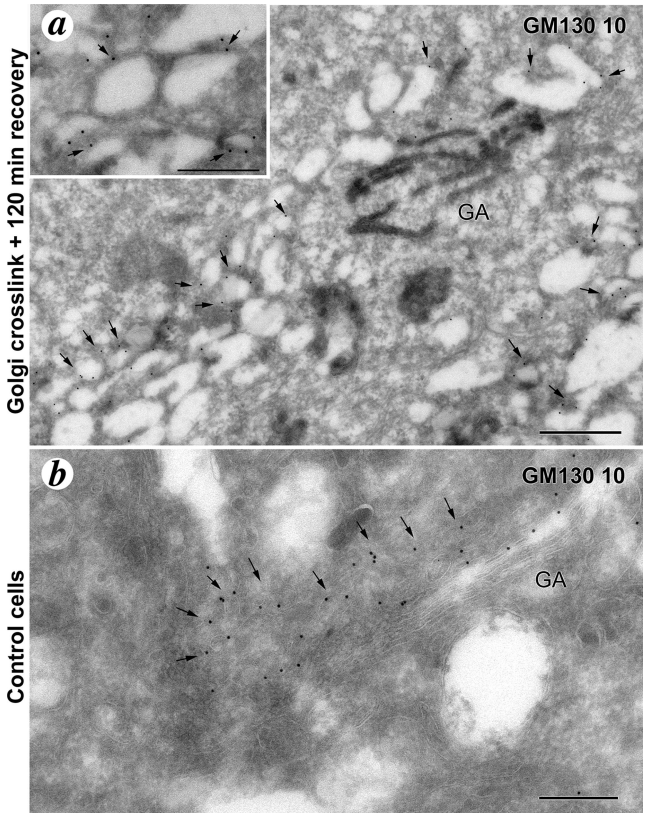

Figure 8. Detection of GM10 by immunoelectron microscopic observation of cells after Golgi cross-linking. ManII-HRP HeLa cells cross-linked by DAB+H_2O_2 and allowed to recover for 120 min (a) or control ManII-HRP HeLa cells treated by H_2O_2 alone (b) were processed for cryoelectron microscopy and immunogold labeling using an anti-GM130 antibody (some gold particles are indicated by an arrow). In cross-linked cells, GM130 is detected on membrane structures, apposed to the inactivated cisternae, that do not display the normal shape of a Golgi complex. This is in marked contrast with the Golgi localization of GM130 observed in non–cross-linked HeLa cells (b). Bar, 500 nm.

specific inactivation. We observed that expression-based enzymatic organelle inactivation is endowed with the same level of specificity as previously described endocytic methods and represents a new tool to specifically perturb organelle function and dynamics.

One key question in cell biology is how are organelles inherited in mitosis and maintained in interphase. Can they form de novo or is "partitioning/replication" the rule? In the case of the Golgi complex, the question is particularly intriguing because organelle maintenance has to be considered in the context of the particular Golgi architecture and of the impressive flux of lipids and proteins transiting through the Golgi stacks in a bidirectional way. Two competing models have been proposed to explain intra-Golgi trafficking: according to the "static cisternae" model a stable Golgi structure receives, modifies, and sorts incoming cargos; in the "cisternal maturation" model that cargos are packed into Golgi cisternae that will progress in the direction of transport, stepwise maturing to acquire enzymes and markers of the next transportation stage (Beznoussenko and Mironov, 2002).

Most studies have addressed the question of Golgi reformation in the context of cell division, which also led to competing models (Roth, 1999; Zaal *et al.*, 1999; Jokitalo *et al.*, 2001; Shorter and Warren, 2002; Barr, 2004). Interestingly, although interphase Golgi complex dynamics seem to be better described by the cisternal maturation model, which predicts efficient neo-formation of Golgi structures, the model most commonly used to describe its re-formation at mitosis exit is based on the fusion of pre-existing Golgi elements and does not rely on auto-organization. This may indicate that the mechanisms responsible for interphase Golgi apparatus growth and replication are different from the mechanisms responsible for its re-formation at the end of cell division.

We therefore asked the question of Golgi maintenance in interphase and analyzed how cells recover from Golgi inactivation and in particular whether a new Golgi apparatus can re-form de novo. Interestingly, new Golgi-like elements formed soon after Golgi cross-linking. We found that these structures are positive for newly synthesized secretory proteins, suggesting that they formed, at least partly, from the ER/intermediate compartment that migrated toward the MTOC area. However, these newly formed Golgi-like structures remain immature, both morphologically and functionally, which agrees with what was observed before in cytoplasts that lack the Golgi apparatus (Pelletier *et al.*, 2000). First, these Golgi-like structures are incompetent for anterograde trafficking because VSV-G was not able to reach the plasma membrane and was not glycosylated by Golgi-specific enzymes. Second, they are not shaped like the mature organelle. No Golgi stacks were observed but, instead, enlarged vacuolar-like structures positive for GM130 were often detected. Third, although they are positive for most Golgi markers (see Table 1), important proteins like giantin or GS15 are missing.

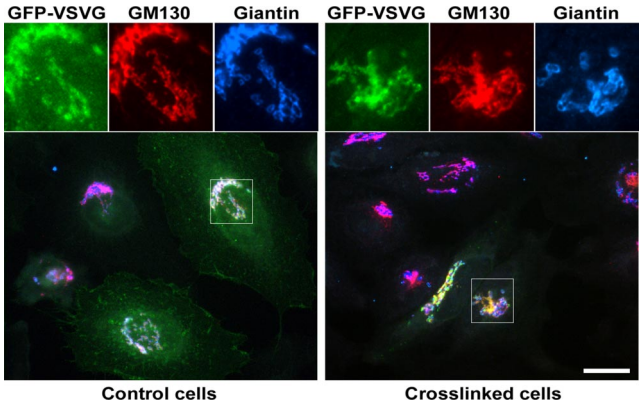

Figure 9. Newly synthesized VSV-G accumulates in the re-formed Golgi-like structure after Golgi cross-linking. HeLa ManII-HRP expressing GFP-VSV-G^{ts045} blocked in the ER at the nonpermissive temperature overnight were treated (right panels) or not (left panels) with DAB/H_2O_2 before being shifted at the permissive temperature for 1 h. Cells were then fixed, permeabilized, and stained using anti-GM130 (red) and anti-giantin (blue) antibodies. The region boxed in the micrographs is shown enlarged above the pictures. In nontreated cells (left), the fraction of VSV-G proteins that did not reach the plasma membrane were found in a compartment positive for GM130 and giantin. In contrast, in cross-linked cells VSV-G proteins localized to a GM130-positive but giantin-negative compartment reminiscent of the newly formed Golgi-like compartment observed in Figure 4. Bar, 20 μm.

The lack of giantin on these newly formed structures is reminiscent of its absence in dispersed mini-Golgi elements formed during nocodazole treatment (Nizak *et al.*, 2003). This is particularly interesting because these elements were shown to be new Golgi apparatus formed from the ER after nocodazole addition (Cole *et al.*, 1996; Storrie *et al.*, 1998). However, when observed by EM, and in contrast with newly formed Golgi-like structures that we report here, they were shown to be composed of apposed cisternae, forming stacks very similar to normal Golgi, albeit less extended (Cole *et al.*, 1996). This suggests that giantin is a marker of mature Golgi but is not necessary for stack apposition (see also Puthenveedu and Linstedt, 2001). Its absence from re-formed Golgi-like structures is thus unlikely to be responsible for the observed morphology defects. In contrast, because giantin has been implicated in COPI-dependent anterograde trafficking (Alvarez *et al.*, 2001; Short *et al.*, 2005), its lack may participate in the trafficking defects that we observed in these Golgi-like structures.

The other important marker missing on newly formed immature Golgi-like structures is GS15. Interestingly, its partners YKT6, GS18, and syntaxin5 (Xu *et al.*, 2002) were detected on these structures indicating that although the t-SNAREs were able to reach the newly formed Golgi-like elements, the v-SNARE GS15 was not. This is surprising because Xu *et al.* (2002) found that GS15 is essential to ensure proper localization of the other members of the complex. However, it has been observed that these proteins can be localized on different structures. Volchuk *et al.* (2004) reported that, although syntaxin 5 and GS28 are homogeneously distributed across the Golgi apparatus, GS15 concentration increases toward the *trans* side. In addition, Tai *et al.* (2004) showed that, upon perturbation of recycling endosomes, GS15 can be trapped on endosomes, whereas syntaxin 5 and GS28 are still Golgi localized. Similarly we observed that after Golgi inactivation syntaxin 5 and GS28 can recycle to the newly formed Golgi-like structures, whereas GS15 cannot.

This would probably affect the function of what Volchuk *et al.* (2004) called the *trans*-SNAREpin, and it is thus tempting to speculate that a key step necessary to re-form a mature and functional Golgi apparatus would involve this complex. A first possibility, as proposed by Volchuk *et al.* (2004) is that *cis*-SNAREpin (not containing GS15) and *trans*-SNAREpin are sequentially active during anterograde transport. Both steps would be necessary to ensure proper Golgi maturation and function, and because only *cis*-SNAREpins would be active after Golgi ablation, an immature Golgi-like structure would be formed. Another possibility takes into account that the *trans*-SNAREpin is involved in retrograde trafficking (Tai *et al.*, 2004). Mature Golgi formation may thus rely on anterograde and retrograde countercurrent membrane flow (see Volchuk *et al.*, 2004). To test these hypotheses, it will be interesting to inactivate GS15 and analyze by EM the structure of the dispersed Golgi apparatus obtained under these conditions (Xu *et al.*, 2002). In addition, it will be important to test whether the re-formed Golgi-like structures can be reached by the GS15-dependent retrograde cargo Shiga toxin B subunit.

Altogether, our results suggest the following model for Golgi complex formation and maturation. The ER generates membranes, containing cargo en route to the Golgi-like VSV-G. These elements are recognized by microtubule minus-end–directed motors and move toward the center of the cell. Golgi peripheral proteins like GMAP210 or GM130 bind to these newly formed membranes, and at least a fraction of these proteins recycle from pre-existing Golgi elements. By themselves, these proteins cannot build functional and mature Golgi because re-forming Golgi generated after HRP-based inactivation are not transport-competent and are not normally shaped. Then, these immature Golgi elements acquire key factors (like GS15) that are presumably transported back to the newly formed Golgi structures from older Golgi cisternae, possibly in a membrane-based, ER-independent retrograde pathway. This will ensure efficient intra-Golgi transport (sequential and/or countercurrent flows), which is essential for the re-forming Golgi to acquire its normal apposed and flattened structure and to become transportation-competent. Whether morphology and activity are functionally linked is still unknown but will now be investigated using the Golgi inactivation system. Finally, additional factors reach the Golgi apparatus via the ER in an anterograde manner, upon neo-synthesis or after slow, ER-dependent recycling. This may be the case for giantin or newly synthesized proteins and possibly for TGN46 that appears on re-forming Golgi structures later than GM130.

In conclusion, the new organelle inactivation system that we describe here will be invaluable to study the function and dynamics of membrane-bound organelles. It allowed us to propose a two-phase integrative model for interphase Golgi complex formation where cargo-containing membranes emanating from the ER mature and acquire Golgi proteins in a stepwise manner, but will not organize as morphologically normal and active Golgi complexes until they receive material from, or fuse with, the pre-existing Golgi elements, hence suggesting that one needs a functional Golgi apparatus to make a new one.

ACKNOWLEDGMENTS

The authors thank Martin Sachse (Institut Pasteur), the imaging staff of the Cell Biology Department of the Institut Curie, Pierre Cosson (Centre Médicale Universitaire, Geneva, Switzerland) for his input at the beginning of this study and for interesting discussions and Joanne Young and Ole Vielemeyer (Institut Curie) for carefully reading and commenting on the manuscript. This work was supported by the Centre National de la Recherche Scientifique and

the Institut Curie. R.S. was supported by a fellowship from Dior-LVMH (Paris, France).

REFERENCES

Altan-Bonnet, N., Sougrat, R., and Lippincott-Schwartz, J. (2004). Molecular basis for Golgi maintenance and biogenesis. Curr. Opin. Cell Biol. *16*, 364–372.

Alvarez, C., Garcia-Mata, R., Hauri, H. P., and Sztul, E. (2001). The p115-interactive proteins GM130 and giantin participate in endoplasmic reticulum-Golgi traffic. J. Biol. Chem. *276*, 2693–2700.

Ang, A. L., Taguchi, T., Francis, S., Folsch, H., Murrells, L. J., Pypaert, M., Warren, G., and Mellman, I. (2004). Recycling endosomes can serve as intermediates during transport from the Golgi to the plasma membrane of MDCK cells. J. Cell Biol. *167*, 531–543.

Axelsson, M. A., and Warren, G. (2004). Rapid, endoplasmic reticulum-independent diffusion of the mitotic Golgi haze. Mol. Biol. Cell *15*, 1843–1852.

Barr, F. A. (2004). Golgi inheritance: shaken but not stirred. J. Cell Biol. *164*, 955–958.

Beznoussenko, G. V., and Mironov, A. A. (2002). Models of intracellular transport and evolution of the Golgi complex. Anat. Rec. *268*, 226–238.

Brachet, V., Pehau-Arnaudet, G., Desaymard, C., Raposo, G., and Amigorena, S. (1999). Early endosomes are required for major histocompatibility complex class II transport to peptide-loading compartments. Mol. Biol. Cell *10*, 2891–2904.

Cole, N. B., Sciaky, N., Marotta, A., Song, J., and Lippincott-Schwartz, J. (1996). Golgi dispersal during microtubule disruption: regeneration of Golgi stacks at peripheral endoplasmic reticulum exit sites. Mol. Biol. Cell *7*, 631–650.

Connolly, C. N., Futter, C. E., Gibson, A., Hopkins, C. R., and Cutler, D. F. (1994). Transport into and out of the Golgi complex studied by transfecting cells with sDNAs encoding horseradish peroxydase. J. Cell Biol. *127*, 641–652.

Cosson, P., Amherdt, M., Rothman, J. E., and Orci, L. (2002). A resident Golgi protein is excluded from peri-Golgi vesicles in NRK cells. Proc. Natl. Acad. Sci. USA 12831–12834.

Futter, C. E., Pearse, A., Hewlett, L. J., and Hopkins, C. R. (1996). Multivesicular endosomes containing internalized EGF-EGF receptor complexes mature and then fuse directly with lysosomes. J. Cell Biol. *132*, 1011–1023.

Glick, B. S. (2002). Can the Golgi form de novo? Nat. Rev. Mol. Cell Biol. *3*, 615–619.

Gurskaya, N. G., Verkhusha, V. V., Shcheglov, A. S., Staroverov, D. B., Chepurnykh, T. V., Fradkov, A. F., Lukyanov, S., and Lukyanov, K. A. (2006). Engineering of a monomeric green-to-red photoactivatable fluorescent protein induced by blue light. Nat. Biotechnol. *24*, 461–465.

Jasmin, B. J., Cartaud, J., Bornens, M., and Changeux, J. P. (1989). Golgi apparatus in chick skeletal muscle: changes in its distribution during end plate development and after denervation. Proc. Natl. Acad. Sci. USA *86*, 7218–7222.

Jokitalo, E., Cabrera-Poch, N., Warren, G., and Shima, D. T. (2001). Golgi clusters and vesicles mediate mitotic inheritance independently of the endoplasmic reticulum. J. Cell Biol. *154*, 317–330.

Jordan, M., Schallhorn, A., and Wurm, F. M. (1996). Transfecting mammalian cells: optimization of critical parameters affecting calcium-phosphate precipitate formation. Nucleic Acids Res. *24*, 596–601.

Karnovsky, M. J. (1971). Use of ferrocyanide-reduced osmium tetroxide in electron microscopy. Proc. 11th Meet. Am. Soc. Cell Biol. Abstr. *284*, 146.

Ladinsky, M. S., Mastronarde, D. N., McIntosh, J. R., Howell, K. E., and Staehelin, L. A. (1999). Golgi structure in three dimensions: functional insights from the normal rat kidney cell. J. Cell Biol. *144*, 1135–1149.

Losev, E., Reinke, C. A., Jellen, J., Strongin, D. E., Bevis, B. J., and Glick, B. S. (2006). Golgi maturation visualized in living yeast. Nature *441*, 1002–1006.

Martinez-Menarguez, J. A., Prekeris, R., Oorschot, V. M., Scheller, R., Slot, J. W., Geuze, H. J., and Klumperman, J. (2001). Peri-Golgi vesicles contain retrograde but not anterograde proteins consistent with the cisternal progression model of intra-Golgi transport. J. Cell Biol. *155*, 1213–1224.

Matsuura-Tokita, K., Takeuchi, M., Ichihara, A., Mikuriya, K., and Nakano, A. (2006). Live imaging of yeast Golgi cisternal maturation. Nature *441*, 1007–1010.

Mironov, A. A., Beznoussenko, G. V., Polishchuk, R. S., and Trucco, A. (2005). Intra-Golgi transport: a way to a new paradigm? Biochim. Biophys. Acta *1744*, 340–350.

Nizak, C., Martin-Lluesma, S. M., Moutel, S., Roux, A., Kreis, T. E., Goud, B., and Perez, F. (2003). Recombinant antibodies selected against subcellular fractions to track endogenous protein dynamics in vivo. Traffic *7*, 739–753.

Nizak, C., Rambourg, A., Jollivet, F., Goud, B., and Perez, F. (2004). Golgi inheritance under a block of anterograde and retrograde traffic. Traffic *5*, 284–299.

Pecot, M. Y., and Malhotra, V. (2004). Golgi membranes remain segregated from the endoplasmic reticulum during mitosis in mammalian cells. Cell *116*, 99–107.

Pecot, M. Y., and Malhotra, V. (2006). The Golgi apparatus maintains its organization independent of the endoplasmic reticulum. Mol. Biol. Cell *17*, 5372–5380.

Pelham, H. R. (2001). Traffic through the Golgi apparatus. J. Cell Biol. *155*, 1099–1101.

Pelletier, L., Jokitalo, E., and Warren, G. (2000). The effect of Golgi depletion on exocytic transport. Nat. Cell Biol. *2*, 840–846.

Pond, L., and Watts, C. (1999). Functional early endosomes are required for maturation of major histocompatibility complex class II molecules in human B lymphoblastoid cells. J. Biol. Chem. *274*, 18049–18054.

Puri, S., and Linstedt, A. D. (2003). Capacity of the golgi apparatus for biogenesis from the endoplasmic reticulum. Mol. Biol. Cell *14*, 5011–5018.

Puthenveedu, M. A., and Linstedt, A. D. (2001). Evidence that Golgi structure depends on a p115 activity that is independent of the vesicle tether components giantin and GM130. J. Cell Biol. *155*, 227–238.

Puthenveedu, M. A., and Linstedt, A. D. (2005). Subcompartmentalizing the Golgi apparatus. Curr. Opin. Cell Biol. *17*, 369–375.

Rabouille, C., and Klumperman, J. (2005). Opinion: the maturing role of COPI vesicles in intra-Golgi transport. Nat. Rev. Mol. Cell Biol. *6*, 812–817.

Rambourg, A., and Clermont, Y. (1997). Three dimensional structure of the Golgi apparatus in mammalian cells. In: The Golgi Apparatus, ed. E.G. Berger and J. Roth, Basel, Switzerland: Birkhäuser, 37–61.

Raposo, G., Kleijmeer, M. J., Posthuma, G., Slot, J. W., and Geuze, H. J. (1997). Immunogold labeling of ultrathin cryosections: application in immunology. In: Handbook of Experimental Immunology, eds. L. A. Herzenberg, D. Weir, and C. Blackwell, Cambridge, MA: Blackwell Science, 1–11.

Roth, M. G. (1999). Inheriting the Golgi. Cell *99*, 559–562.

Sheff, D., Pelletier, L., O'Connell, C. B., Warren, G., and Mellman, I. (2002). Transferrin receptor recycling in the absence of perinuclear recycling endosomes. J. Cell Biol. *156*, 797–804.

Shima, D. T., Haldar, K., Pepperkok, R., Watson, R., and Warren, G. (1997). Partitioning of the Golgi apparatus during mitosis in living HeLa cells. J. Cell Biol. *137*, 1211–1228.

Short, B., Haas, A., and Barr, F. A. (2005). Golgins and GTPases, giving identity and structure to the Golgi apparatus. Biochim. Biophys. Acta *1744*, 383–395.

Shorter, J., and Warren, G. (2002). Golgi architecture and inheritance. Annu. Rev. Cell Dev. Biol. *18*, 379–420.

Stinchcombe, J. C., Nomoto, H., Cutler, D. F., and Hopkins, C. R. (1995). Anterograde and retrograde traffic between the rough endoplasmic reticulum and the Golgi complex. J. Cell Biol. *131*, 1387–1401.

Storrie, B. (2005). Maintenance of Golgi apparatus structure in the face of continuous protein recycling to the endoplasmic reticulum: making ends meet. Int. Rev. Cytol. *244*, 69–94.

Storrie, B., White, J., Rottger, S., Stelzer, E. H., Suganuma, T., and Nilsson, T. (1998). Recycling of golgi-resident glycosyltransferases through the ER reveals a novel pathway and provides an explanation for nocodazole-induced Golgi scattering. J. Cell Biol. *143*, 1505–1521.

Tai, G., Lu, L., Wang, T. L., Tang, B. L., Goud, B., Johannes, L., and Hong, W. (2004). Participation of the syntaxin 5/Ykt6/GS28/GS15 SNARE complex in transport from the early/recycling endosome to the trans-Golgi network. Mol. Biol. Cell *15*, 4011–4022.

Volchuk, A. *et al.* (2004). Countercurrent distribution of two distinct SNARE complexes mediating transport within the Golgi stack. Mol. Biol. Cell *15*, 1506–1518.

Warren, G., and Wickner, W. (1996). Organelle inheritance. Cell *84*, 395–400.

Xu, Y., Martin, S., James, D. E., and Hong, W. (2002). GS15 forms a SNARE complex with syntaxin 5, GS28, and Ykt6 and is implicated in traffic in the early cisternae of the Golgi apparatus. Mol. Biol. Cell *13*, 3493–3507.

Xu, Y., Wong, S. H., Zhang, T., Subramaniam, V. N., and Hong, W. (1997). GS15, a 15-kilodalton Golgi soluble N-ethylmaleimide-sensitive factor attachment protein receptor (SNARE) homologous to rbet1. J. Biol. Chem. *272*, 20162–20166.

Yoshimura, S.-i., Nakamura, N., Barr, F. A., Misumi, Y., Ikehara, Y., Ohno, H., Sakaguchi, M., and Mihara, K. (2001). Direct targeting of cis-Golgi matrix proteins to the Golgi apparatus. J. Cell Sci. *114*, 4105–4115.

Zaal, K. J. *et al.* (1999). Golgi membranes are absorbed into and reemerge from the ER during mitosis. Cell *99*, 589–601.